Journal of Medicinal Chemistry

Article

pubs.acs.org/jmc

Development of a Mucin4-Targeting SPIO Contrast Agent for Effective Detection of Pancreatic Tumor Cells in Vitro and in Vivo

Shou-Cheng Wu,[†] Yu-Jen Chen,[†] Yi-Jan Lin,[‡] Tung-Ho Wu,[§] and Yun-Ming Wang*[,†,∥]

[†]Department of Biological Science and Technology, Institute of Molecular Medicine and Bioengineering, National Chiao Tung University, 75 Bo-Ai Street, Hsinchu 300, Taiwan

[‡]Graduate Institute of Natural Products and Center of Excellence for Environmental Medicine, Kaohsiung Medical University, Kaohsiung 807, Taiwan

[§]Division of Cardiovascular Surgery, Veterans General Hospital, Kaohsiung, 813, Taiwan

[∥]Department of Biomedical Science and Environmental Biology, Kaohsiung Medical University, Kaohsiung 807, Taiwan

Supporting Information

ABSTRACT: In search of a unique and reliable contrast agent targeting pancreatic adenocarcinoma, new multifunctional nanoparticles (MnMEIO-silane-NH_2-(MUC4)-mPEG NPs) were successfully developed in this study. Mucin4-expression levels were determined through different imaging studies in a panel of pancreatic tumor cells (HPAC, BxPC-3, and Panc-1) both in vitro and in vivo studies. The in vitro T_2-weighted MR imaging study in HPAC and Panc-1 tumor cells treated with NPs showed −89.1 ± 5.7% and −0.9 ± 0.2% contrast enhancement, whereas in in vivo study, it is found to be −81.5 ± 4.5% versus −19.6 ± 5.2% (24 h postinjection, 7.0 T), respectively. The T_2-weighted MR and optical imaging studies revealed that the novel contrast agent can specifically and effectively target to mucin4-expressing tumors in nude mice. Hence, it is suggested that MnMEIO-silane-NH_2-(MUC4)-mPEG NPs are able to provide an efficient and targeted delivery of MUC4 antibodies to mucin4-expressing pancreatic tumors.

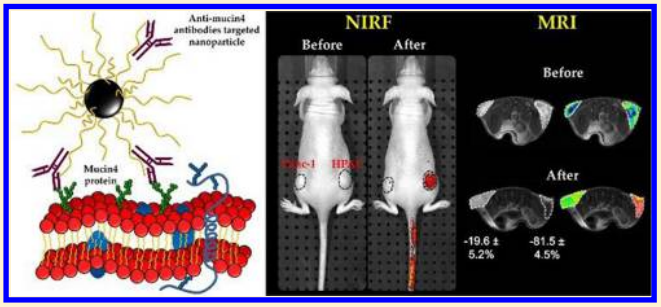

INTRODUCTION

Magnetic resonance imaging (MRI) is one of the most widely used diagnostic techniques in medical applications.[1,2] MRI offers several advantages over others, including high spatial resolution, noninvasiveness, high anatomical contrast, and no harmful radiation.[3] MRI can provide biological information and functions at preclinical stages.[4] Cancer is one of the major diseases and claims nearly 25% of deaths annually.[5] Among them, pancreatic cancer is a devastating disease with incidence increasing at an alarming rate and survival rate has not been improved substantially during the past few decades. It is the fourth leading cause of death among all cancers in USA, with a dismal 5-year survival rate of less than 5%.[6] Although enormous efforts have been attempted for early detection and comprehensive treatment of this disease, little or no survival improvement was obtained. Having made little progress in early diagnosis of pancreatic tumors using traditional techniques, a paradigm shift in our approach to develop imaging agents and diagnostic methods for detecting this tumor at an early pre-symptomatic stage is urgently required.

Advances in nanomedicine have resulted in rapid development of a variety of nanomaterials as emerging tools in tumor diagnostic and treatment.[7−9] Future trends for early detection, individual therapy, and prognostic monitoring of pancreatic tumors are now focusing on multifunctional nanomedicines. Emerging inorganic nanomaterials, such as carbon nanotubes, quantum dots,[10] and mesoporous silica[11] /gold/supermagnetic nanoparticles, have been widely used in biomedical research with great optimism for tumor diagnosis and therapy owing to their interesting physical features such as unique optical, electrical, magnetic, and/or electrochemical properties. To enhance NP's capability of targeting a specific tumor, target-specific ligands or antibodies will be good candidates to be attached onto the nanoparticulate surface, thus allowing the drugs to be directed to the specific cell for the desirable action in low doses.[12] In this regard, targeted NPs can be considered as suitable vehicles for site-specific delivery and protection barriers, as reagents encapsulated inside NPs prevent their untimely degradation during intravenous administration, thereby increasing their therapeutic competence.

MUC4 antibody was chosen as the potential targeting moiety due to overexpression of mucin4, a member of the epidermal growth factor receptors (EGFRs) family, on the pancreatic tumor cells. Mucins (MUCs) are heavily glycosylated, high molecular weight glycoproteins with an aberrant expression profile in various malignancies. Research report has shown that mucin4 protein, a member of the membrane-bound mucin gene

Received: July 14, 2013
Published: October 22, 2013

dx.doi.org/10.1021/jm401060z | J. Med. Chem. 2013, 56, 9100−9109

Table 1. Hydrodynamic Size, ζ Potential, and Relaxivities (r_1 and r_2) of MnMEIO-silane-NH_2-mPEG and MnMEIO-silane-NH_2-(MUC4)-mPEG NPs

	hydrodynamic size (nm)	ζ potential (mV)	r_1 (mM^{-1} s^{-1})	r_2 (mM^{-1} s^{-1})	r_2/r_1
MnMEIO-silane-NH_2-mPEG	39.3 ± 2.2	+17.3 ± 2.3	35.7 ± 1.5	239.7 ± 5.9	7.9
MnMEIO-silane-NH_2-(MUC4)-mPEG	55.9 ± 5.6	−4.3 ± 0.5	30.1 ± 1.3	216.1 ± 4.4	5.7

family, is a high molecular weight *O*-glycoprotein produced by secretory epithelial cells for the lubrication and protection of ducts and lumen.[13] Previous study showed that mucin4 was detected in 11 of 15 (73%) of the pancreatic cancer cell lines and in 12 of 16 (75%) of the clinical samples and remained undetectable in any of the chronic pancreatitis tissue and normal pancreatic cell lines. This indicates that mucin4 is overexpressed in pancreatic tumor cells but is undetectable in normal pancreas and chronic pancreatitis.[14] Functional studies on mucin4 have provided substantial evidence for its role in the promotion of pancreatic tumor cells growth and metastasis,[15,16] as knock-down of mucin4-expression reduced pancreatic tumor cells growth and metastasis. It has been shown that overexpression of the cell-surface mucin4 disrupts integrin-mediated cell adhesions as well as the homotypic cell−cell interactions, causing the dissociation of tumor cells in culture.[17] Consistent with these observations, previous studies have raised future hopes that mucin4 could be a good candidate of tumor marker for early diagnosis of pancreatic cancer, in which mucin4 exhibits 91% sensitivity and 100% specificity.[18]

Early reports have described the synthesis of monocrystalline iron oxide (MION) with cholecystokinin, a peptide hormone that acts as a bioactive targeting moiety by binding with a G-protein coupled receptor expressed on pancreatic acinar cells,[19] and developed strepavidin−MION conjugates to image pancreatic tumor cells by targeting secretin receptors on pancreatic acinar cells.[20] Recently, an iron oxide-based MR contrast agent conjugated with single-chain anti-EGFR antibodies for the detection of pancreatic tumor cells has also been reported.[21] After administration, the contrast agent was internalized in EGFR-expressing pancreatic tumor cells, providing 5-fold reduction in the MR signal. A reverse "negative" targeting strategy was used for MR imaging of an animal model of pancreatic ductal adenocarcinoma (PDAC).[22]

To the best of our knowledge, we are the first to successfully use MUC4 antibodies conjugated nanoparticles for tumor diagnosis in vivo, and the result warrants further exploration of these nanomaterials for tumor therapeutic applications. We believe this study will help define the design parameters to formulate better strategies for specifically targeting tumors with nanoparticle conjugates. The objective of this study is to develop MUC4 antibodies loaded MnMEIO-silane-NH_2-mPEG NPs for early pancreatic tumor cells detection. MUC4 antibodies were functionalized and conjugated to the surface of MnMEIO-silane-NH_2-mPEG NPs to achieve preferential receptor mediated targeting to pancreatic tumor cells. The well-differentiated cell line, HPAC, that expresses high level of mucin4 protein and the moderately or poorly differentiated cell lines, BxPC-3 and Panc-1, are used for the in vitro study here.[23,24] In vitro and in vivo efficacy of all the reagents (i.e., free NPs and MUC4 antibodies conjugated NPs) were evaluated through flow cytometry analysis, confocal fluorescent microscopic studies, MR imaging, and optical imaging studies.

RESULTS AND DISCUSSION

Characterization of MR-Optical Imaging Agents. It is known that there exists an electrostatic interaction between the NPs and negatively charged cell membranes and such an interaction is capable of preventing specific binding.[25] To promote the specific binding, the amine group can be entangled inside the mPEG chains, which is used as an insulator. This can reduce the electrostatic interaction between NPs and negatively charged cell membranes and enhance the specific binding (Supporting Information Figure S1). On the basis of this silane-NH_2-mPEG, coated NPs (MnMEIO-silane-NH_2-mPEG NPs) were prepared through a ligand-exchange reaction using oleic acid, oleyl amine-stabilized MnMEIO NPs, and silane-NH_2-mPEG. Silane-NH_2-mPEG was synthesized via Michael addition of *N*-Boc-ethylenediamine to methoxypoly (ethylene glycol) acrylate (mPEG-Ac) and Boc deprotection to (3-aminopropyl) triethoxy silane acrylate (APTES-Ac) (Supporting Information Scheme S1). The compounds (**1**, **2**, silane-NBoc-EA-mPEG, and silane-NH_2-mPEG) were further analyzed by HPLC for confirming the purity (≥95%) (Supporting Information Figure S2A−D). Successful ligand exchange reaction was confirmed by Fourier transform infrared spectroscopy (FT-IR). Size distributions of MnMEIO core of MnMEIO NPs, MnMEIO-silane-NH_2-mPEG NPs, and MnMEIO-silane-NH_2-(MUC4)-mPEG NPs were obtained by TEM analyses. The final compound (MnMEIO-silane-NH_2-(MUC4)-mPEG NPs) was analyzed by HPLC to confirm the purity (≥95%) (Supporting Information Figure S2E). As shown in Supporting Information Figure S3, the TEM analyses revealed that the core size of MnMEIO NPs was in the average diameter of 7.6 ± 0.2 nm (Supporting Information Figure S3A). By comparing TEM images of modified NPs (Supporting Information Figure S3B,C), the core sizes of NPs were consistent with MnMEIO NPs. These TEM images indicated that the modified NPs formed during polymerization and antibody conjugation resembled the MnMEIO NPs. Furthermore, these NPs exhibit a well-dispersed property. The hydrodynamic size of MnMEIO-silane-NH_2-mPEG NPs and MnMEIO-silane-NH_2-(MUC4)-mPEG NPs were verified by dynamic light-scattering (DLS). The DLS measurement studies showed that MnMEIO-silane-NH_2-mPEG NPs have a relatively narrow size distribution with a mean size of 39.3 ± 2.2 nm (Supporting Information Figure S3D). Upon conjugation with Cy777 and MUC4 antibody, the size of the NPs increased to about 55.9 ± 5.6 nm (Supporting Information Figure S3E). Previous work demonstrated that the length of one single antibody is approximately 7.5 nm.[26] Therefore, this thickness of the NPs enlarged assumed that two to three MUC4 antibodies conjugation per nanoparticle. Furthermore, the ζ potential values of MnMEIO-silane-NH_2-mPEG NPs and MnMEIO-silane-NH_2-(MUC4)-mPEG NPs are found to be +17.3 ± 2.3 and −4.3 ± 0.5 mV, respectively. This result indicated that the ζ potential value found for MnMEIO-silane-NH_2-mPEG NPs was dropped for MnMEIO-silane-NH_2-(MUC4)-mPEG NPs at pH 7.0, and this decrease can be attributed to the conjugation of MUC4 antibodies to amine groups. The negative ζ potential value (−4.3 ± 0.5 mV)

dx.doi.org/10.1021/jm401060z | J. Med. Chem. 2013, 56, 9100−9109

obtained for MnMEIO-silane-NH_2-(MUC4)-mPEG NPs may support their specific binding to mucin4-expression tumor cells. The relaxivities (r_1 and r_2) of the MnMEIO-silane-NH_2-(MUC4)-mPEG NPs measured at 20 MHz and 37.0 ± 0.1 °C were found to be 35.7 ± 1.5 and 216.1 ± 4.4 mM^{-1} s^{-1}, respectively (Table 1). Moreover, the loading capacity of MUC4 antibody in NPs measured by NanoDrop ND-1000 UV−vis spectrometer was found to be 93.4 μg/mg NPs. The NPs obtained by the current synthetic route are characterized by a good dispersion, a narrow size distribution, and excellent magnetic properties.

The T_2-Weighted MR Imaging Study of MnMEIO-silane-NH_2-(MUC4)-mPEG NPs. To assess whether the nanoparticles (MnMEIO-silane-NH_2-(MUC4)-mPEG NPs and MnMEIO-silane-NH_2-mPEG NPs) could be used as contrast agents for MRI, T_2-weighted MR images were performed in a 7.0 T MRI system. The measurements were carried out at different iron concentrations (0.06, 0.13, 0.25, and 0.50 mM). The calculation of negative contrast enhancements of the nanoparticles was determined by comparing their results to that of Resovist, a commercial available standard. Figure 1 clearly showed the negative contrast enhancement

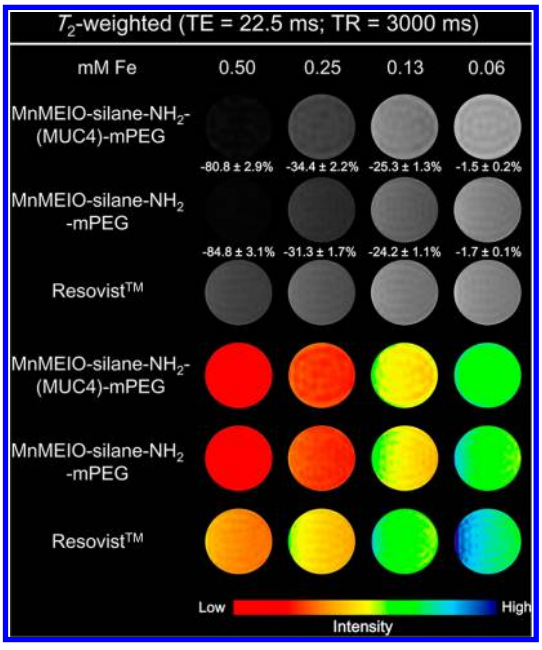

Figure 1. The T_2-weighted MR images of MnMEIO-silane-NH_2-(MUC4)-mPEG, MnMEIO-silane-NH_2-mPEG, and Resovist at different Fe concentrations (mM).

effect on T_2-weighted images of nanoparticles (MnMEIO-silane-NH_2-(MUC4)-mPEG NPs and MnMEIO-silane-NH_2-mPEG NPs) and Resovist at different Fe concentrations. Interestingly, we have observed that the negative contrast enhancements were increased with the increase of Fe concentrations. Moreover, nanoparticles conjugated with antibodies (MnMEIO-silane-NH_2-(MUC4)-mPEG) showed similar negative contrast enhancements to those nanoparticles without MUC4 antibodies conjugation (MnMEIO-silane-NH_2-mPEG) within the range of Fe concentrations studied. These results proved that nanoparticles containing MUC4 antibody and free nanoparticles possessed similar effects and that MUC4 antibodies conjugation with nanoparticles would not interfere with the MR images. Furthermore, the above-mentioned nanoparticles showed better negative contrast enhancements than that of commercial Resovist.

Determination of Mucin4 Protein Expression Levels in Pancreatic Tumor Cells. To determine the mucin4-expression level in the pancreatic tumor cells, Western blot assay was conducted with pancreatic HPAC, BxPC-3, and Panc-1 tumor cells, and β-actin was used as an internal control. As shown in Figure 2, mucin4 protein (MW = 135 kDa)

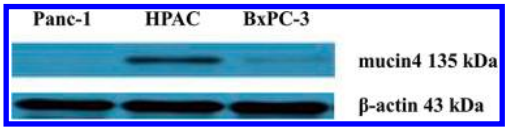

Figure 2. Western blotting assay of mucin4 protein expression level in HPAC, BxPC-3, and Panc-1 tumor cells.

expression level was significantly increased in HPAC and slightly upregulated in BxPC-3, whereas it was not expressed in Panc-1. For the further determination of mucin4-expression level in the pancreatic tumor cells, MUC4 antibody binding efficiency was studied through flow cytometry analysis (Figure 3). Next, the FITC moiety was conjugated with MUC4

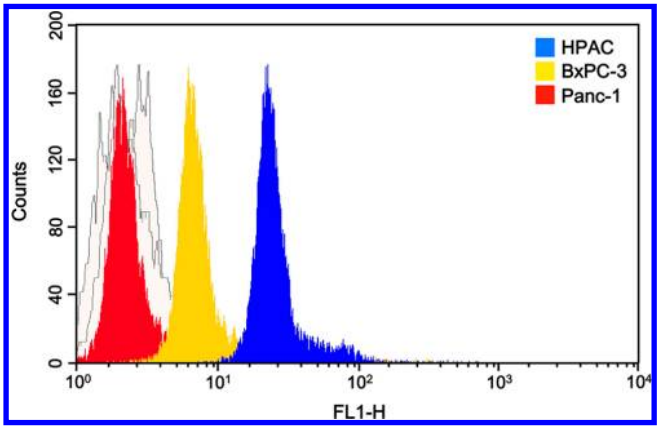

Figure 3. Specificity of fluorescein-conjugated MUC4 antibodies: FACS profiles for the tagging affinities of MUC4 antibodies toward the tumor cells with varied mucin4-expression levels.

antibody to provide fluorescent signal for the flow cytometry analysis. In the experiments, MUC4-FITC was incubated with HPAC, BxPC-3, and Panc-1 tumor cells at 37 °C for 1 h. The results showed that the highest fluorescence intensity from HPAC tumor cells represented the highest mucin4-expression level as compared to that from BxPC-3 and Panc-1 tumor cells. These results are consistent with an earlier report that Panc-1 cell lacks mucin4-expression due to histone deacetylation.[17] These studies indicated that the HPAC and BxPC-3 tumor cells exhibited mucin4-expression and are suitable for further analyses. Panc-1 tumor cells with almost nil mucin4-expression can be used as control.

In Vitro MR Imaging Study. To demonstrate the binding specificity of MnMEIO-silane-NH_2-(MUC4)-mPEG NPs in tumor cells, in vitro MR imaging studies were performed in a 7.0 T MRI system. The pancreatic tumor cells (HPAC and BxPC-3) and the control cells (Panc-1) were treated with MnMEIO-silane-NH_2-(MUC4)-mPEG NPs and MnMEIO-silane-NH_2-mPEG NPs at the Fe concentration of 10 μg/mL, respectively, and the scale of corresponding MR negative contrast enhancement was quantified. The results of in vitro T_2-

dx.doi.org/10.1021/jm401060z | J. Med. Chem. 2013, 56, 9100−9109

weighted MR images observed for free nanoparticles (MnMEIO-silane-NH_2-mPEG NPs) showed negative contrast enhancements −7.8 ± 1.1%, −9.3 ± 0.8%, and −0.7 ± 0.1% in HPAC, BxPC-3, and Panc-1 cells, respectively, while the nanoparticles conjugated with MUC4 antibodies exhibited −89.1 ± 5.7%, −69.5 ± 3.3%, and −0.9 ± 0.2% in HPAC, BxPC-3, and Panc-1 cells, respectively. These results indicated that the free nanoparticles, MnMEIO-silane-NH_2-mPEG NPs, cannot specifically bind to both pancreatic tumor cells (HPAC and BxPC-3) and control cells (Panc-1), whereas the highly binding specificity was observed in MUC4 antibody conjugated nanoparticles. On the other hand, the intensity of negative contrast enhancement was marked in the HPAC tumor cells in which mucin4 level was highly expressed, whereas Panc-1 tumor cells, with lower mucin4-expression, showed a significantly lower negative contrast enhancement (Figure 4).

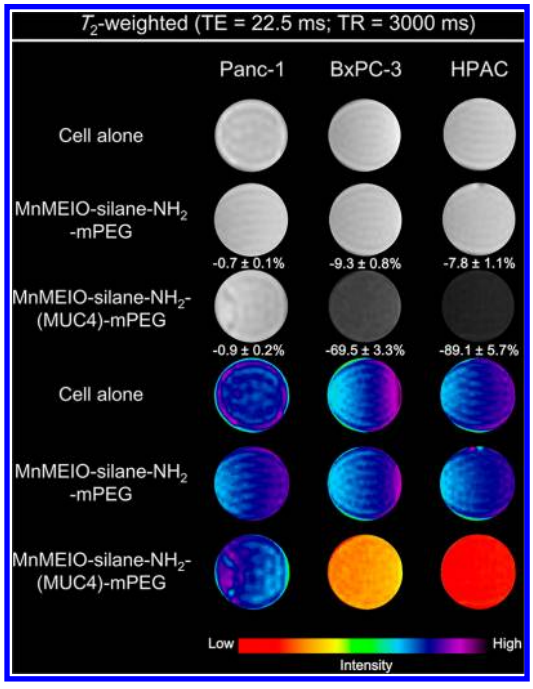

Figure 4. In vitro T_2-weighted MR images of MnMEIO-silane-NH_2-(MUC4)-mPEG and MnMEIO-silane-NH_2-mPEG at the Fe concentrations of 10 μg/mL on HPAC, BxPC-3, and Pan-1 tumor cells.

Flow Cytometry and Confocal Fluorescence Imaging Analysis. To further characterize the in vitro specificity of MnMEIO-silane-NH_2-(MUC4)-mPEG NPs in pancreatic tumor cells, the cellular uptake was studied through flow cytometry analysis (Supporting Information Figure S4). The FITC moiety was used to provide the fluorescent signal in flow cytometry analysis. In the tumor cells uptake experiments, MnMEIO-silane-NH_2-(MUC4)-mPEG NPs were incubated at 37 °C for 1 h with HPAC, BxPC-3, and Panc-1 tumor cells. The results indicated that HPAC tumor cells exhibiting higher mucin4-expression showed higher fluorescence intensity as compared to that of BxPC-3 tumor cells with lower mucin4-expression. By comparison, Panc-1 showed only a very slight change in its fluorescence intensity, which further proved its least expressing mucin4 level. All these facts suggested that NPs can bind to HPAC and BxPC-3 tumor cells and differentiate mucin4-expressing levels. In contrast, the Panc-1 tumor cells did not show any binding with NPs.

The flow cytometry results were supported by immunofluorescence staining in which pancreatic tumor cells and the control cells were incubated with the contrast agent, MnMEIO-silane-NH_2-(MUC4)-mPEG NPs at 37 and 4 °C (Figure 5 and

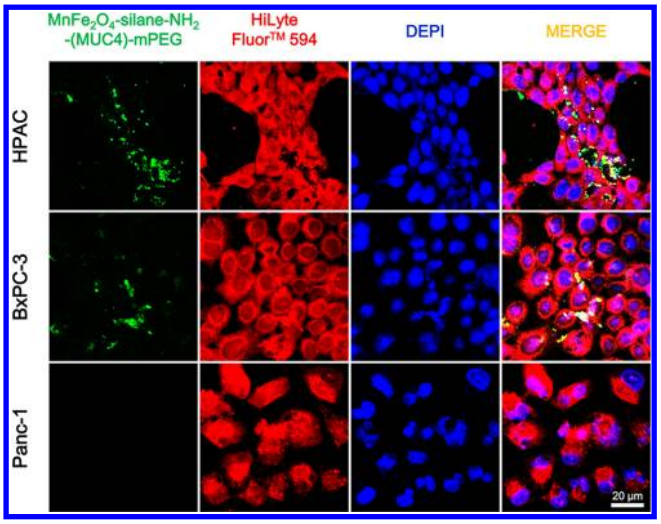

Figure 5. Confocal microscopy images of pancreatic tumor cells incubated with MnMEIO-silane-NH_2-(MUC4)-mPEG NPs (10 μg/mL) for 4 h at 37 °C. Cytoplasm (stained with HiLyte Fluor 594 in red), nuclei (stained with DEPI in blue).

Supporting Information Figure S5). Figure 5 showed substantial variations of FITC fluorescence signals observed for HPAC, BxPC-3, and Panc-1 tumor cells at 37 °C. Although all three tested cells showed green fluorescence signal, the green fluorescence intensity observed in HPAC and BxPC-3 tumor cells was clearly stronger than that found in Panc-1 tumor cells. This result can be referred to higher mucin4-expressing level of HPAC and BxPC-3 tumor cells than that of Panc-1 tumor cells. In addition, the same experiments were also performed at 4 °C to confirm the targeting capability of MUC4 antibody (Supporting Information Figure S5). In this experiment, the green fluorescence was observed only in HPAC and BxPC-3 tumor cells but not in Panc-1 tumor cells. These results are consistent with the confocal experimental study carried out at 37 °C, and the similar results were further demonstrated by Prussian blue staining experiments (Supporting Information Figure S6). These results confirmed that the uptake of the NPs by tumor cells was via receptor-mediated internalization.

In Vivo Optical Imaging and Biodistribution Studies. The optical imaging capability of MnMEIO-silane-NH_2-(MUC4)-mPEG NPs and MnMEIO-silane-NH_2-mPEG NPs was also investigated to detect mucin4-expression in tumors. Typical whole body fluorescent images of nude mice bearing subcutaneous tumor xenografts of HPAC and Panc-1 tumor cells at different time points after the intravenous injection of MnMEIO-silane-NH_2-(MUC4)-mPEG and MnMEIO-silane-NH_2-mPEG NPs were shown in Figure 6. After 1 h postinjection, a strong fluorescence enhancement was observed in mice bearing HPAC tumor cells and its fluorescence image persists for up to 96 h with a gradual attenuation in signal intensity, whereas the fluorescence enhancement was not observed in mice with the Panc-1 tumor cells. Furthermore, the fluorescence images of dissected organs from experimental mice after 24 h postinjection of MnMEIO-silane-NH_2-(MUC4)-mPEG NPs were acquired for detailed examination. Figure 6C

dx.doi.org/10.1021/jm401060z | J. Med. Chem. 2013, 56, 9100−9109

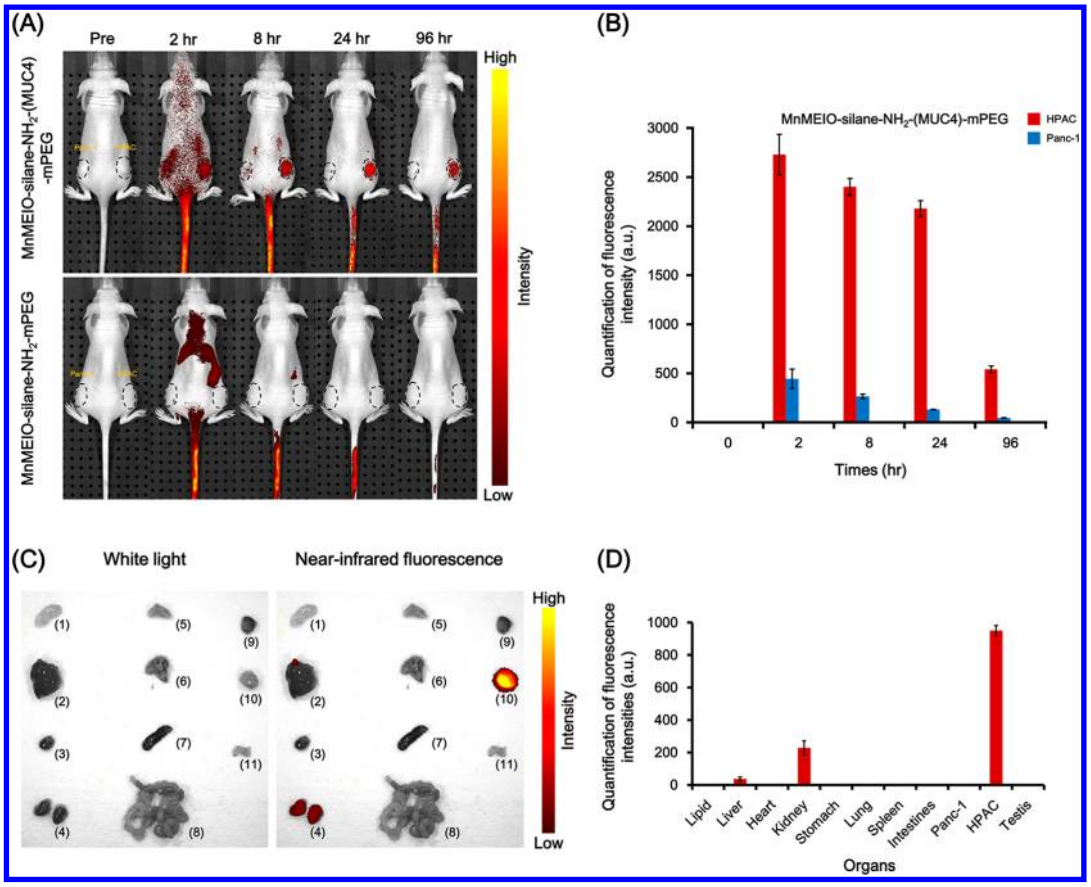

Figure 6. (A) In vivo optical images of nude mice bearing subcutaneous tumor xenografts of HPAC and Panc-1 tumor cells after intravenous injection of MnMEIO-silane-NH_2-(MUC4)-mPEG NPs and MnMEIO-silane-NH_2-mPEG NPs (10 mg/kg). (B) Quantitative fluorescent intensities of the NPs in the tumors with images acquired at preinjection and various time points (2, 8, 24, and 96 h) postinjection. (C) In vivo white light and near-infrared fluorescence images of dissected organs of mice bearing HPAC and Panc-1 tumors sacrificed after 24 h postinjection of MnMEIO-silane-NH_2-(MUC4)-mPEG NPs (10 mg/kg) (excitation, 745 nm; emission, 820 nm). (1) Lipid, (2) liver, (3) heart, (4) kidney, (5) stomach, (6) lung, (7) spleen, (8) intestines, (9) Panc-1 tumor, (10) HPAC tumor, and (11) testis. (D) Quantification of fluorescence intensities of isolated organs.

showed that significant fluorescence intensity was observed in HPAC tumor, and a moderate intensity was detected in kidney. In contrast, Panc-1 tumor showed no significant signal. In agreement with the in vivo optical imaging studies, HPAC tumor showed a strong fluorescence signal and the strong signals shown in the fluorescence images were resulted from the specific binding of MnMEIO-silane-NH_2-(MUC4)-mPEG NPs to the mucin4-expressing tumors. All the above experiments suggested that MnMEIO-silane-NH_2-(MUC4)-mPEG NPs can serve as an efficient and specific target probe for the identification of mucin4-expressing tumor (HPAC).

In Vivo MR Imaging Study. It has been shown that overexpression of mucin4 does not affect the level of EGFR receptor expression in either HPAC or Panc-1 tumor cell lines, but it does reduce binding affinity of a number of anti-EGFR antibodies, including Erbitux and Herceptin.[27]

Thus, MUC4 antibodies which conjugated on MnMEIO-silane-NH_2-mPEG NPs are specific and reliable tumor associated molecular markers. It is also known that the overexpression of mucin4 has been typically observed in pancreatic tumor cells but not in normal pancreas and chronic pancreatitis.[14] Earlier reports showed that mucin4 serves as a marker to identify the pancreatic intraepithelial neoplasia lesions in clinical samples[15] and the spontaneous pancreatic tumor progression in mouse models.[28]

On the basis of these facts, in vivo MR imaging study was carried out for MnMEIO-silane-NH_2-(MUC4)-mPEG NPs using nude mice bearing subcutaneous tumor xenografts of HPAC, BxPC-3, and Panc-1 tumor cells in lateral thighs. MnMEIO-silane-NH_2-(MUC4)-mPEG NPs was administrated at 10 mg/kg by intravenous injection, and MR image was measured using T_2-weighted fast spin−echo sequence 7.0 T/1.0 T imaging. The results of in vivo MR images of HPAC and Panc-1 were shown in Figures 7 and 8. The negative contrast enhancements (24 h postinjection) of HPAC tumor cells were about −81.5 ± 4.5% (7.0 T) and −80.5 ± 4.3% (1.0 T). In comparison of the HPAC and Panc-1 tumor images, the negative contrast enhancements were −81.5 ± 4.5% versus −19.6 ± 5.2% (24 h postinjection, 7.0 T) and −80.5 ± 4.3% versus −4.7 ± 2.2% (24 h postinjection, 1.0 T), respectively. Moreover, the results of in vivo optical images and in vivo MR images, as shown in Figures 6 and 7, also indicated that MnMEIO-silane-NH_2-(MUC4)-mPEG NPs can clearly distinguish HPAC and Panc-1 tumors after 8 h postinjection in both optical and MR images.

Similar results of T_2-weighted MR images (7.0 T/1.0 T) were observed on nude mice bearing subcutaneous xenografts of HPAC and BxPC-3 tumor cells before and after injection of MnMEIO-silane-NH_2-(MUC4)-mPEG NPs (10 mg/kg) (Supporting Information Figures S7 and S8). By comparing these

dx.doi.org/10.1021/jm401060z | J. Med. Chem. 2013, 56, 9100−9109

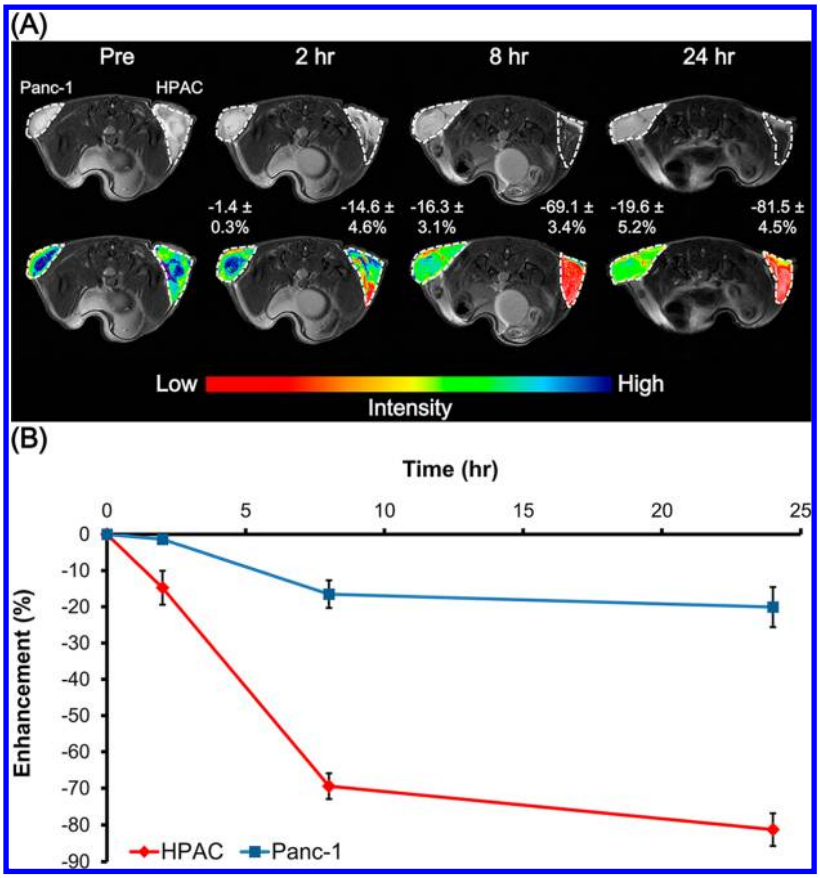

Figure 7. (A) T_2-weighted MR images (7.0 T) of nude mice bearing subcutaneous tumor xenografts of HPAC (right) and Panc-1 (left) tumor cells before and after injection of MnMEIO-silane-NH_2-(MUC4)-mPEG (10 mg/kg). (B) Quantitative fluorescent intensities of the NPs in the tumors. Images were acquired at preinjection and 2, 8, and 24 h of postinjection.

results, it is clear that high negative contrast enhancement observed for HPAC tumor cells indicated more accumulation of contrast agents, and moderate or slight negative contrast enhancements observed for BxPC-3 or Panc-1 tumor cells, respectively, indicated moderate or little accumulation of contrast agents.

CONCLUSION

In summary, we have successfully developed the nanoparticles, MnMEIO-silane-NH_2-(MUC4)-mPEG NPs containing a targeting moiety, MUC4 antibodies, as a unique dual-modality MR-optical imaging contrast agent. This contrast agent possessed the ability to specifically target the mucin4-expressing tumor cells. In this study, we have demonstrated that MnMEIO-silane-NH_2-(MUC4)-mPEG NPs can sensitively and specifically target pancreatic tumor cells. We believe our results may provide an ideal MR-optical imaging contrast agent for early diagnosis of human pancreatic tumors.

EXPERIMENTAL SECTION

Materials. Iron(III) acetylacetonate ([$Fe(acac)_3$], 99.9%), manganese(II) chloride ($MnCl_2 \cdot 4H_2O$, 99%), methyl poly(ethylene glycol) (mPEG, MW = 2,000), oleic acid (90%), oleylamine (90%), *N*-ethyl-*N*′-(3-dimethylaminopropyl) carbodiimide (EDC), IR-783, fluorescein isothiocyanate (FITC), Prussian blue, and anti-mucin4 antibodies (MUC4) were purchased from Sigma-Aldrich (St. Louis, MO, USA). Acryloyl chloride (96%) and *N*-Boc-ethylenediamine (98%) were purchased from Alfa Aesar (Ward Hill, MA, USA). (3-Aminopropyl) triethoxy silane (APTES, 98%) and benzyl ether were purchased from Fluka (Buchs, SG, Switzerland). (Benzotriazol-1-yloxy) tripyrrolidinophosphonium hexafluorophosphate (PyBOP) and *N*-hydroxybenzotriazole (HOBt) were purchased from NovaBiochem (Beeston, NTH, UK). BCA (bicinchoninic acid) protein assay reagent kit was purchased from Pierce (Rockford, IL, USA). Molecular-porous membrane tubing (MW = 12−14 kDa and MW = 50 kDa) was purchased from Spectrum (Houston, TX, USA). Matrigel was purchased from BD Bioscience (Bedford, MA, USA). All chemicals were used directly without any further purification unless otherwise stated.

Methods. The FT-IR analyses were performed using a Perkin-Elmer spectrum 2000 Fourier transform infrared spectrometer (Boston, MA, USA). The ^1H NMR (300 MHz) spectra were recorded on a Varian Unity-300 NMR spectrometer (Palo Alto, CA, USA). HPLC analysis was performed on Waters 2695 Alliance system (Milford, MA, USA) coupled with Varian PL Aquagel−OH column (300 mm × 7.5 mm; particle size 20 μm) (Palo Alto, CA, USA) and Waters 2420 ELS detector. The mobile phase composition was a mixture of methanol−water (10: 90, v/v). The EDS spectra of MnMEIO and MnMEIO-silane-NH_2-mPEG NPs were obtained on a Hitachi S-3000N energy-dispersive spectrometer (Chiyoda-ku, TYO, Japan). Relaxation time values (T_1 and T_2) of aqueous solutions of MnMEIO-silane-NH_2-(MUC4)-mPEG NPs were measured to determine the relaxivities r_1 and r_2. All measurements were made at 20 MHz and 37.0 ± 0.1 °C using a Bruker NMS-120 Minispec relaxometer (Milton, ON, Canada). Hydrodynamic size and ζ potential were analyzed with a Malvern Instruments DLS Nano ZS90 (Malvern, WOR, UK). Protein concentration was determined with a NanoDrop ND-1000 UV−vis spectrometer (Wilmington, DE, USA). The flow cytometry experiments were carried out using a FACScan flow cytometer (San Jose, CA, USA). The confocal fluorescent studies were performed using a Olympus Fluoview 300 imaging system consisting of an Olympus BX51 microscope (Chiyoda-

dx.doi.org/10.1021/jm401060z | J. Med. Chem. 2013, 56, 9100−9109

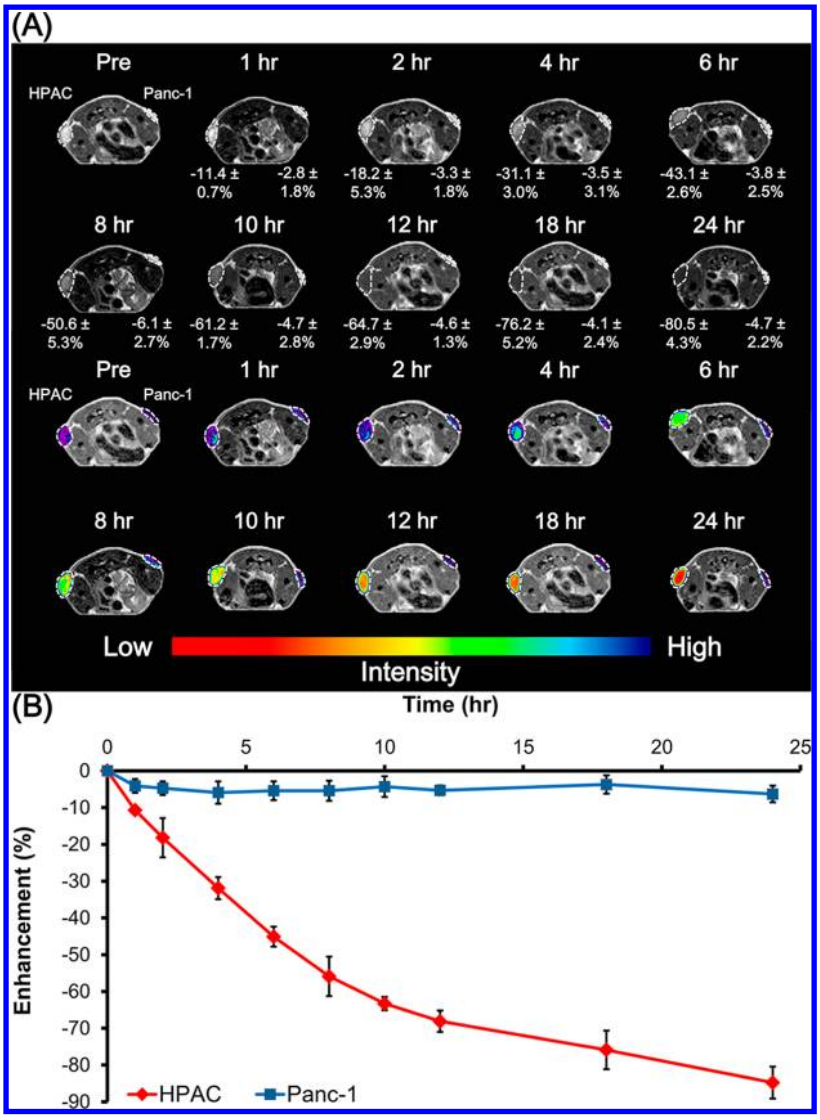

Figure 8. (A) T_2-weighted MR images (1.0 T) of nude mice bearing subcutaneous tumor xenografts of HPAC (left) and Panc-1 (right) tumor cells before and after injection of MnMEIO-silane-NH_2-(MUC4)-mPEG NPs (10 mg/kg). (B) Quantitative fluorescent intensities of the NPs in the tumors. Images were acquired at preinjection and 1, 2, 4, 6, 8, 10, 12, 18, and 24 h postinjection.

ku, TYO, Japan) and a 20 mW output 488 nm argon ion laser. The MR imaging was performed on an Aspect Imaging 1.0 T M2 compact high-performance MRI system (Toronto, ON, Canada) and Bruker 7.0 T MRI system (Ettlingen, Germany) with a volume coil used as radio frequency (RF) transmitter and receiver. Optical imaging were acquired using an IVIS spectrum system (Hopkinton, MA, USA), and images collected were analyzed by Xenogen living image software version 3.0 (Hopkinton, MA, USA).

Synthesis of Cy777. The Cy777 dye was prepared according to the literature report.[29] To a solution of IR-783 (250 mg, 0.33 mmol) in 6 mL of anhydrous DMF was added 3-mercaptopropionic acid (40.7 μL, 0.47 mmol) and TEA (65.3 μL, 0.47 mmol). The green solution was allowed to stir in the dark for 21 h, and the completion of the reaction was monitored by HPLC. A green solid was isolated by precipitation with cold ether and washed with cold ether (3 mL). The precipitations were dissolved in water and dried under vacuum (214 mg, 81.5% yield). ^{1}H NMR (300 MHz, CD_3OD) δ (ppm): 1.76 (s, 12H), 2.00−1.92 (m, 10H), 2.56 (t, 2H, J = 6.9 Hz), 2.71 (t, 4H, J = 5.9 Hz), 2.90−2.87 (m, 4H), 3.10 (t, 2H, J = 7.0 Hz), 4.20 (t, 4H, J = 6.7 Hz), 6.30 (d, 2H, J = 14.3 Hz), 7.26 (t, 2H, J = 7.5 Hz), 7.33 (d, 2H, J = 7.8 Hz), 7.41 (t, 2H, J = 7.6 Hz), 7.48 (d, 2H, J = 7.4 Hz), 8.87 (d, 2H, J = 14.2 Hz). ESI-MS m/z calcd for $C_{41}H_{51}N_2O_8S_3$ 795.3, found 795.5.

Synthesis of Fluorescein-Conjugated MUC4 Antibodies. FITC (0.01 mg, 0.03 μmol) was dissolved in DMSO (1 mL), and the mixture with 20 μL of MUC4 antibodies (1 mg/mL) was stirred overnight at 4 °C. Subsequently, the free FITC and DMSO were removed by dialysis (MW = 50 kDa) against deionized water.

Synthesis of MnMEIO-silane-NH_2-mPEG NPs. MnMEIO NPs were prepared according to the literature report[1] using iron acetylacetonate and manganese chloride as the iron and manganese precursor, respectively, oleic acid and oleylamine as the ligands, and benzyl ether as the solvent. The silane-NH_2-mPEG was prepared according to Supporting Information Scheme S1. The compounds (**1**, **2**, silane-NBoc-EA-mPEG, and silane-NH_2-mPEG) were further analyzed by HPLC for confirming the purity (≥95%). The silane-NH_2-mPEG stabilized NPs, MnMEIO-silane-NH_2-mPEG NPs, were obtained by ligand exchange reaction. In the typical ligand exchange reaction, synthesized MnMEIO NPs (56 mg, 0.24 mmol) was dispersed in toluene (20 mL) in a round-bottom flask, followed by the addition of silane-NH_2-mPEG (600 mg, 0.24 mmol). The resulting solution was sonicated for 6 h at 50 °C. The silane-NH_2-mPEG coated NPs were precipitated by addition of hexane and isolated via centrifugation (1000g). After decanting the supernatant, the precipitate was redispersed in hexane for three times. Then, the particle was dispersed in deionized water and purified by dialysis (MW = 50 kDa)

dx.doi.org/10.1021/jm401060z | J. Med. Chem. 2013, 56, 9100−9109

against deionized water. Selected IR bands (ν in cm^{-1}): 3100−3700 (−OH and $-NH_2$), 2884 ($-CH_2$), 2820 ($-CH_3$), 1693 (C═O), 1410 (CH_2-COO^-), 1247 ($-CH_2$ and Si−C), 1202 ($-OCH_3$), 1177 (C−N), 1170−1000 (Si−O-R), 1110 (C−O−C), 1034 (C−O−C), 592 (Fe−O).

Synthesis of MnMEIO-silane-NH_2-(MUC4)-mPEG NPs. Cy777 (0.8 mg, 1.00 μmol) and EDC (0.38 mg, 1.98 μmol) were dissolved in DMSO (5 mL) and allowed to react for 20 min at room temperature. Subsequently, MnMEIO-silane-NH_2-mPEG NPs (100 mg), dispersed in deionized water (5 mL), were added and vigorously shaken for overnight at room temperature in the dark. Excess EDC were removed by centrifugation (1000g) for three times and dialyzed against deionized water (MW = 12−14 kDa). After purification, MnMEIO-silane-NH_2-mPEG (100 mg) and 20 μL of MUC4 antibodies (1 mg/mL) were dissolved in DMSO (5 mL) and the solution added with PyBOP and HOBT overnight to obtain the MnMEIO-silane-NH_2-(MUC4)-mPEG NPs. Free PyBOP, HOBT, and DMSO were removed by dialysis (MW = 12−14 kDa) against PBS buffer. The final compound (MnMEIO-silane-NH_2-(MUC4)-mPEG NPs) was analyzed by HPLC for confirming the purity (≥95%) using an Aquagel−OH column (300 mm × 7.5 mm; particle size 20 μm) and ELS detector. The mobile phase composition was a mixture of methanol−water (10: 90, v/v). Then, MnMEIO-silane-NH_2-(MUC4)-mPEG NPs (100 μmol of manganese ferrite) were dissolved in coating buffer (0.05 M sodium carbonate and 0.1 M sodium bicarbonate). The amount of antibody was determined by UV−vis spectrometry with background correction from a solution of MnMEIO-silane-NH_2-mPEG of equal concentration according to the Warburg's eq 1[4]

$$c(\mathrm{mg/mL}) = 1.55 \times (A_{280} - A_{320}) - 0.76 \times (A_{260} - A_{320}) \quad (1)$$

where c is the protein concentration calculated from the absorbance at the indicated wavelengths and A is the absorbance. The NPs used in flow cytometry and confocal fluorescent microscopy studies were prepared by following the same procedure as mentioned above by replacing Cy777 with FITC.

Determination of Conjugation Efficiency of Anti-Mucin4 Antibodies Associated with NPs. The conjugation efficiency between MUC4 antibodies with MnMEIO-silane-NH_2-mPEG NPs was determined by collecting unconjugated oligonucleotides in the supernatant after centrifugal filtration of the MUC4 antibodies reaction mixture and measuring the concentration using NanoDrop ND-1000 UV−vis spectrometer. Data are represented as mean ± SD (n = 4).

The T_2-Weighted MR Images of Contrast Agents. The contrast agents, MnMEIO-silane-NH_2-mPEG and MnMEIO-silane-NH_2-(MUC4)-mPEG NPs were prepared with different concentration of Fe (0.06, 0.13, 0.25, and 0.50 mM) and scanned by a fast gradient echo pulse sequence (7.0T) using Resovist as a standard contrast agent. The data is represented as mean ± SD (n = 4). The contrast enhancement (%) was calculated by the following eq 2

$$\mathrm{enhancement}(\%) = (\mathrm{SI}_{\mathrm{experiment}} - \mathrm{SI}_{\mathrm{control}})/\mathrm{SI}_{\mathrm{control}} \times 100 \quad (2)$$

where $SI_{experiment}$ is the value of signal intensity of difference concentration of Fe (0.06, 0.13, 0.25, and 0.50 mM) for contrast agents (MnMEIO-silane-NH_2-mPEG, and MnMEIO-silane-NH_2-(MUC4)-mPEG NPs) and $SI_{control}$ is the value of signal intensity of commercial product Resovist alone.

Western Blot Assay. The primary antibodies used here were MUC4 (1:200 dilution) and anti β-actin (1:5000 dilution). Cells were washed twice with cold PBS buffer and lysed on ice in RIPA buffer (10 mM PBS, 1% NP40, 0.1% sodium dodecyl sulfate (SDS), 5 mM EDTA, 0.5% sodium deoxycholate, and 1 mM sodium orthovanadate) with the presence of protease inhibitors and quantified using NanoDrop ND-1000 UV−vis spectrometer. Equal amount of protein (50−80 μg) was separated by SDS polyacrylamide gel, electro-transferred to polyvinylidene fluoride membranes (PVDF), and blocked in 5% nonfat dry milk in pH 7.5 Tris-buffer (100 mM NaCl, 50 mM Tris, 0.1% Tween-20). Membranes were immuno-blotted overnight at 4 °C with MUC4 monoclonal antibodies and anti-β-actin, followed by their respective horseradish peroxidase conjugated secondary antibodies. Signals were detected by enhanced chemiluminescence. The β-actin was used as the internal control.

Cells and Animal Model. Mucin4 protein expressing tumor cells (HPAC and BxPC-3) and non-mucin4-expressing tumor cell (Panc-1) were cultured in DMEM/F12, RPMI, and DMEM medium, respectively, and supplemented with 10% fetal bovine serum (FBS) (GIBCO). All cells were cultured in a humidified incubator at 37 °C with 5% CO_2.

BALB/cAnN.Cg-Foxn1nu/CrlNarl mice (6−8 weeks old, female) were purchased from the National Laboratory Animal Center, Taipei, Taiwan. Animal experiments were performed in accordance with the institutional guidelines. HPAC, BxPC-3, and Panc-1 tumor cells were subcutaneously injected to the flanks of nude mice (n = 4) in 100 μL (1×10^6 cells) of PBS with matrigel. MR imaging experiments were performed two weeks after tumor implantation, at which time the tumors were measured approximately 500 mm^3 in volume. Data is represented as mean ± SD (n = 4).

Flow Cytometry. HPAC, BxPC-3, and Panc-1 tumor cells were collected in microcentrifuge tubes (1×10^6 cells each). These tumor cells were incubated with 1 μg/mL of fluorescein-conjugated MUC4 antibodies or MnMEIO-silane-NH_2-(MUC4)-mPEG NPs (10 μg/mL) for 1 h at 37 °C, washed three times in PBS, and then resuspended by 1 mL of PBS in FACS tube. Finally, the immunofluorescence of viable cells was measured and their fluorescent intensity was analyzed with the BD Bioscience CELLQUEST software (Bedford, MA, USA).

In Vitro MR Imaging Study. All tumor cells (HPAC, BxPC-3, and Panc-1) containing 1×10^6 cells were incubated with MnMEIO-silane-NH_2-mPEG and MnMEIO-silane-NH_2-(MUC4)-mPEG NPs (10 μg/mL) for 1 h at 37 °C and washed three times in PBS, respectively. All samples were scanned by a fast gradient echo pulse sequence (7.0 T), and data are represented as mean ± SD (n = 4). The contrast enhancement (%) was calculated by the following eq 3

$$\mathrm{enhancement}(\%) = (\mathrm{SI}_{\mathrm{post}} - \mathrm{SI}_{\mathrm{pre}})/\mathrm{SI}_{\mathrm{pre}} \times 100 \quad (3)$$

where SI_{post} is the value of signal intensity of tumor cells treated with the contrast agents, MnMEIO-silane-NH_2-mPEG or MnMEIO-silane-NH_2-(MUC4)-mPEG NPs, and SI_{pre} is the value of signal intensity of tumor cells untreated.

Confocal Fluorescent Microscopy. All tumor cells (HPAC, BxPC-3, and Panc-1) were seeded at a density of 2×10^5 cells/well on cover glasses (24 mm × 24 mm) and allowed to grow for 24 h. Then tumor cells were incubated with MnMEIO-silane-NH_2-(MUC4)-mPEG NPs (10 μg/mL) for 4 h at 37 °C and 1 h at 4 °C, washed three times with PBS, and fixed with 4% formaldehyde solution for 30 min at room temperature. Cell nuclei and cytoplasm were stained with 4′-6-diamidino-2-phenylindole (DAPI, blue) and HiLyte Fluor 594 acid (red), respectively. Cover glasses containing fixed cells were mounted in a mixture of PBS and glycerol (1:1) on a microscope slide, and the cells were observed using confocal imaging system.

Prussian Blue Stain Assay. All tumor cells (HPAC, BxPC-3, and Panc-1) were seeded at a density of 2×10^5 cells/well on cover glasses (24 mm × 24 mm) and allowed to grow for 24 h. Then tumor cells were incubated with MnMEIO-silane-NH_2-(MUC4)-mPEG NPs (10 μg/mL) for 1 h at 4 °C. Slides were stained with Prussian blue to detect Fe deposition. Briefly, hypodermic tumor sections mounted on slides were stained with a 1:1 mixture of 2% potassium ferrocyanide and 2% hydrochloric acid for 30 min at room temperature. The slides were rinsed with PBS buffer, dehydrated, and photographed.

In Vivo Optical Imaging Study. Nude mice bearing HPAC, and Panc-1 tumor cells (approximately 500 mm^3) were anesthetized and injected via tail vein with MnMEIO-silane-NH_2-mPEG and MnMEIO-silane-NH_2-(MUC4)-mPEG NPs (10 mg/kg), respectively. Optical imaging were acquired at preinjection and various time points (2, 8, 24, and 96 h) postinjection using an IVIS spectrum system. Then the emission at 820 nm was measured with an optimal excitation

dx.doi.org/10.1021/jm401060z | J. Med. Chem. 2013, 56, 9100−9109

wavelength of 745 nm (1 s, F-stop = 2 and small binning). Data is represented as mean ± SD (n = 4).

Biodistribution Study. MnMEIO-silane-NH_2-(MUC4)-mPEG NPs (10 mg/kg) were intravenously injected into nude mice bearing HPAC and Panc-1 tumor cells (approximately 500 mm^3). The mice were sacrificed after 24 h of the intravenous injection. Lipid, liver, heart, kidney, stomach, lung, spleen, intestines, testis, Panc-1 tumors, and HPAC tumors were harvested and washed with PBS. The fluorescence signal of organs and tumors were measured by IVIS spectrum system. Then the emission at 820 nm was measured with an optimal excitation wavelength of 745 nm (1 s, F-stop = 2 and small binning). Data is represented as mean ± SD (n = 4).

In Vivo MR Imaging Study. Nude mice bearing HPAC, BxPC-3, and Panc-1 tumor cells (approximately 500 mm^3) were anesthetized by pentobarbital. MnMEIO-silane-NH_2-(MUC4)-mPEG NPs and the control contrast agent (MnMEIO-silane-NH_2-mPEG NPs) (10 mg/kg) were infused via the tail vein to the mice. All mice were measured using a T_2-weighted fast spin−echo sequence 7.0 T/1.0T imaging for every 3 mm sectioning thickness. Images were acquired at preinjection and various time points 2, 8, and 24 h/1, 2, 4, 6, 8, 10, 12, 18, and 24 h postinjection, respectively. Data is represented as mean ± SD (n = 4). The contrast enhancement (%) was calculated by eq 2, where SI_{post} is the value of signal intensity of the tumor cells after contrast agents injection and SI_{pre} is the value of signal intensity of the tumor cells before contrast agents injection.

■ ASSOCIATED CONTENT

Supporting Information

Illustration of MnMEIO-silane-NH_2-(MUC4)-mPEG NPs and specific targeting efficacy by masking positive charges on the NPs, synthetic scheme of silane-NH_2-mPEG, liquid chromatography of compounds **1**, **2**, silane-NBoc-EA-mPEG, and silane-NH_2-mPEG, TEM images of MnMEIO NPs, flow cytometric analysis the specificity of MnMEIO-silane-NH_2-(MUC4)-mPEG NPs, confocal microscopy images of pancreatic tumor cells incubated with NPs for 1 h at 4 °C, Prussian blue staining of pancreatic tumor cells treated with NPs for 4 h at 37 °C, T_2-weighted MR images (7.0 T) of nude mice bearing subcutaneous tumor xenografts of pancreatic tumor cells before and after injection of NPs, T_2-weighted MR images (1.0 T) of nude mice bearing subcutaneous tumor xenografts of pancreatic tumor cells before and after injection of NPs. This material is available free of charge via the Internet at http://pubs.acs.org.

■ AUTHOR INFORMATION

Corresponding Author

*Phone: 886-3-5712121 ext 56972. Fax: 886-3-5729288. E-mail: ymwang@mail.nctu.edu.tw. Address: Department of Biological Science and Technology, Institute of Molecular Medicine and Bioengineering, National Chiao Tung University, 75 Bo-Ai Street, Hsinchu 300, Taiwan.

Author Contributions

The manuscript was written through contributions of all authors. All authors have given approval to the final version of the manuscript.

Notes

The authors declare no competing financial interest.

■ ACKNOWLEDGMENTS

We are grateful to the National Science Council of the Republic of China for financial support under contract no. NSC 101-2627-M-009-006. This research was also particularly supported by "Aim for the Top University Plan" of the National Chiao Tung University and Ministry of Education.

■ ABBREVIATIONS USED

SPIO, superparamagnetic iron oxide; NPs, nanoparticles; MnMEIO, Mn-doped magnetism-engineered iron oxide; MRI, magnetic resonance imaging; EGFR, epidermal growth factor receptor; MUC4, anti-mucin4 antibodies; MUCs, mucins; MION, monocrystalline iron oxide nanoparticles; PDAC, pancreatic ductal adenocarcinoma

■ REFERENCES

(1) Accardoa, A.; Gianoliob, E.; Arenab, F.; Barnertc, S.; Schubertc, R.; Tesauroa, D.; Morelli, G. Nanostructures based on monoolein or diolein and amphiphilic gadolinium complexes as MRI contrast agents. *J. Mater. Chem., B* **2013**, *1*, 617−628.

(2) Laurent, S.; Forge, D.; Port, M.; Roch, A.; Robic, C.; Vander, E. L.; Muller, R. N. Magnetic iron oxide nanoparticles: synthesis, stabilization, vectorization, physicochemical characterizations, and biological applications. *Chem. Rev.* **2008**, *108*, 2064−2110.

(3) Wu, Y. L.; Ye, Q.; Ho, C. Cellular and functional imaging of cardiac transplant rejection. *Curr. Cardiovasc. Imaging Rep.* **2011**, *4*, 50−62.

(4) Kuzucan, A.; Chen, J. H.; Bahri, S.; Mehta, R. S.; Carpenter, P. M.; Fwu, P. T.; Yu, H. J.; Hsiang, D. J.; Lane, K. T.; Butler, J. A.; Feig, S. A.; Su, M. Y. Diagnostic performance of magnetic resonance imaging for assessing tumor response in patients with HER2-negative breast cancer receiving neoadjuvant chemotherapy is associated with molecular biomarker profile. *Clin. Breast Cancer* **2012**, *12*, 110−118.

(5) Ferrari, M. Cancer nanotechnology: opportunities and challenges. *Nature Rev. Cancer* **2005**, *5*, 161−171.

(6) Jemal, A.; Siegel, R.; Ward, E.; Hao, Y.; Xu, J.; Thun, M. J. Cancer statistics 2009. *CA, Cancer J. Clin.* **2009**, *59*, 225−249.

(7) Liu, Z.; Peng, P. Inorganic nanomaterials for tumor angiogenesis imaging. *Eur. J. Nucl. Med. Mol. Imaging* **2010**, *37*, 147−163.

(8) Yezhelyev, M.; Yacoub, R.; O'Regan, R. Inorganic nanoparticles for predictive oncology of breast cancer. *Nanomedicine* **2009**, *4*, 83−103.

(9) Kang, H.; DeLong, R.; Fisher, M. H.; Juliano, R. L. Tat-conjugated PAMAM dendrimers as delivery agents for antisense and siRNA oligonucleotides. *Pharm. Res.* **2005**, *22*, 2099−2106.

(10) Zhang, B.; Gong, X.; Hao, L.; Cheng, J.; Han, Y.; Chang, J. A novel method to enhance quantum yield of silica-coated quantum dots for biodetection. *Nanotechnology* **2008**, *19*, 465604.

(11) Cheng, S. H.; Lee, C. H.; Yang, C. S.; Tseng, F. G.; Mou, C. Y.; Lo, L. W. Mesoporous silica nanoparticles functionalized with an oxygen sensing probe for cell photodynamic therapy: potential cancer theranostics. *J. Mater. Chem.* **2009**, *19*, 1252−1257.

(12) Das, M.; Mohanty, C.; Sahoo, S. K. Ligand-based targeted therapy for cancer tissue. *Expet. Opin. Drug Delivery* **2009**, *6*, 285−304.

(13) Porchet, N.; Nguyen, V. C.; Dufosse, J.; Audie, J. P.; Guyonnet-Duperat, V.; Gross, M. S.; Denis, C.; Degand, P.; Bernheim, A.; Aubert, J. P. Molecular cloning and chromosomal localization of a novel human trachea−bronchial mucin cDNA containing tandemly repeated sequences of 48 base pairs. *Biochem. Biophys. Res. Commun.* **1991**, *175*, 414−422.

(14) Andrianifahanana, M.; Moniaux, N.; Schmied, B. M.; Ringel, J.; Friess, H.; Hollingsworth, M. A.; Buchler, M. W.; Aubert, J. P.; Batra, S. K. Mucin (MUC) gene expression in human pancreatic adenocarcinoma and chronic pancreatitis: a potential role of MUC4 as a tumor marker of diagnostic significance. *Clin. Cancer Res.* **2001**, *7*, 4033−4040.

(15) Swartz, M. J.; Batra, S. K.; Varshney, G. C.; Hollingsworth, M. A.; Yeo, C. J.; Cameron, J. L.; Wilentz, R. E.; Hruban, R. H.; Argani, P. MUC4 expression increases progressively in pancreatic intraepithelial neoplasia. *Am. J. Clin. Pathol.* **2002**, *117*, 791−796.

(16) Singh, A. P.; Moniaux, N.; Chauhan, S. C.; Meza, J. L.; Batra, S. K. Inhibition of MUC4 expression suppresses pancreatic tumor cell growth and metastasis. *Cancer Res.* **2004**, *64*, 622−630.

(17) Singh, A. P.; Chaturvedi, P.; Batra, S. K. Emerging roles of MUC4 in cancer: a novel target for diagnosis and therapy. *Cancer Res.* **2007**, *67*, 433−436.
(18) Jhala, N.; Jhala, D.; Vickers, S. M.; Eltoum, I.; Batra, S. K.; Manne, U.; Eloubeidi, M.; Jones, J. J.; Grizzle, W. E. Biomarkers in diagnosis of pancreatic carcinoma in fine-needle aspirates: a translational research application. *Am. J. Clin. Pathol.* **2006**, *126*, 572−579.
(19) Reimer, P.; Weissleder, R.; Shen, T.; Knoefel, W. T.; Brady, T. J. Pancreatic receptors: initial feasibility studies with a targeted contrast agent for MR imaging. *Radiology* **1994**, *193*, 527−531.
(20) Shen, T. T.; Bogdanov, A., Jr.; Bogdanova, A.; Poss, K.; Brady, T. J.; Weissleder, R. Magnetically labeled secretin retains receptor affinity to pancreas acinar cells. *Bioconjugate Chem.* **1996**, *7*, 311−316.
(21) Yang, L.; Mao, H.; Wang, Y. A.; Cao, Z.; Peng, X.; Wang, X.; Duan, H.; Ni, C.; Yuan, Q.; Adams, G.; Smith, M. Q.; Wood, W. C.; Gao, X.; Nie, S. Single chain epidermal growth factor receptor antibody conjugated nanoparticles for in vivo tumor targeting and imaging. *Small* **2009**, *5*, 235−243.
(22) Montet, X.; Weissleder, R.; Josephson, L. Imaging pancreatic cancer with a peptide−nanoparticle conjugate targeted to normal pancreas. *Bioconjugate Chem.* **2006**, *17*, 905−911.
(23) Perrais, M.; Pigny, P.; Ducourouble, M. P.; Petitprez, D.; Porchet, N.; Aubert, J. P.; Van Seuningen, I. Characterization of human mucin gene MUC4 promoter: importance of growth factors and proinflammatory cytokines for its regulation in pancreatic cancer cells. *J. Biol. Chem.* **2001**, *276*, 30923−30933.
(24) Deer, E. L.; González-Hernández, J.; Coursen, J. D.; Shea, J. E.; Ngatia, J.; Scaife, C. L.; Firpo, M. A.; Mulvihill, S. J. Phenotype and genotype of pancreatic cancer cell lines. *Pancreas* **2010**, *39*, 425−435.
(25) Wu, S. C.; Lin, K. L.; Wang, T. P.; Tzou, S. C.; Singh, G.; Chen, M. H.; Cheng, T. L.; Chen, C. Y.; Liu, G. C.; Lee, T. W.; Hu, S. H.; Wang, Y. M. Imaging specificity of MR-optical imaging agents following the masking of surface charge by poly(ethylene glycol). *Biomaterials* **2013**, *34*, 4118−4127.
(26) Ban, N.; Escobar, C.; Garcia, R.; Hasel, K.; Day, J.; Greenwood, A.; McPherson, A. Crystal structure of an idiotype-anti-idiotype Fab complex. *Proc. Natl. Acad. Sci. U. S. A.* **1994**, *91*, 1604−1608.
(27) Price-Schiavi, S. A.; Jepson, S.; Li, P.; Arango, M.; Rudland, P. S.; Yee, L.; Carraway, K. L. Rat MUC4 (sialomucin complex) reduces binding of anti-Erbb2 antibodies to tumor cell surfaces, a potential mechanism for herceptin resistance. *Int. J. Cancer* **2002**, *99*, 783−791.
(28) Rachagani, S.; Torres, M. P.; Kumar, S.; Haridas, D.; Baine, M.; Macha, M. A.; Kaur, S.; Ponnusamy, M. P.; Dey, P.; Seshacharyulu, P.; Johansson, S. L.; Jain, M.; Wagner, K. U.; Batra, S. K. Mucin (Muc) expression during pancreatic cancer progression in spontaneous mouse model: potential implications for diagnosis and therapy. *J. Hematol. Oncol.* **2012**, *5*, 68−79.
(29) Hilderbrand, S. A.; Kelly, K. A.; Weissleder, R.; Tung, C. H. Monofunctional near-infrared fluorochromes for imaging applications. *Bioconjugate Chem.* **2005**, *16*, 1275−1281.